




Gene tagging via CRISPR-mediated homology-directed repair in cassava

Kira M. Veley ^{1,†} Ihuoma Okwuonu,^{2,‡} Greg Jensen,^{1,†} Marisa Yoder,^{1,†} Nigel J. Taylor,^{1,†} Blake C. Meyers ^{1,3,†} and Rebecca S. Bart ^{1,†,*}

¹Donald Danforth Plant Science Center, Saint Louis, MO 63132, USA

²Biotechnology Research Division, National Root Crops Research Institute, Umudike, Abia State, Nigeria

³Division of Plant Sciences, University of Missouri, Columbia, MO 65211, USA

[†]Present address: Donald Danforth Plant Science Center, Saint Louis, MO 6313

[‡]Present address: National Root Crops Research Institute, Umudike, Abia State, Nigeria

*Corresponding author: Donald Danforth Plant Science Center, Saint Louis, MO, USA. rbart@danforthcenter.org

Abstract

Research on a few model plant–pathogen systems has benefitted from years of tool and resource development. This is not the case for the vast majority of economically and nutritionally important plants, creating a crop improvement bottleneck. Cassava bacterial blight (CBB), caused by *Xanthomonas axonopodis* pv. *manihotis* (*Xam*), is an important disease in all regions where cassava (*Manihot esculenta* Crantz) is grown. Here, we describe the development of cassava that can be used to visualize one of the initial steps of CBB infection *in vivo*. Using CRISPR-mediated homology-directed repair (HDR), we generated plants containing scarless insertion of GFP at the 3' end of CBB susceptibility (*S*) gene *MeSWEET10a*. Activation of *MeSWEET10a-GFP* by the transcription activator-like (TAL) effector TAL20 was subsequently visualized at transcriptional and translational levels. To our knowledge, this is the first such demonstration of HDR via gene editing in cassava.

Keywords: bacterial pathogens; pathogenesis; genome editing; *Xanthomonas*; cassava

Introduction

Many plant pathogens, including bacteria, fungi, oomycetes, and animals, secrete proteins known as effectors into host cells to modulate host defense responses and alter gene expression to benefit the pathogen (Hogenhout *et al.* 2009). Understanding how effectors facilitate pathogenicity at the molecular level is critical for improving resistance and disrupting the processes underlying host colonization and disease. For many bacterial pathogens, effectors play an important role in disease, by targeting and altering specific host molecules (*e.g.*, proteins, RNA, DNA) to benefit the bacteria (Feng and Zhou 2012). Some such interactions are recognized by plant resistance (*R*) genes, resulting in an immune response. A common strategy for improving crop disease tolerance is the introduction of *R* genes into susceptible varieties (Dangl *et al.* 2013). Though effective, this strategy requires the existence or engineering of active *R* genes. Even if a suitable *R* gene is available, this strategy may be overcome by the pathogen (Brown 2015).

Targeting susceptibility (*S*) genes is a viable alternative for engineering disease resistance in plants (Xu *et al.* 2019). *S* genes are typically necessary for normal plant growth and development, but present liabilities within the host's genome which can be exploited by the pathogen to promote virulence (van Schie and Takken 2014). Preventing such exploitation is a goal for

engineering resistance. As with *R* genes, this strategy also requires in-depth, molecular-level knowledge of the relationship between the pathogen and host cells. Many well-characterized *S* gene–effector relationships are described from the model bacterial pathogens *Pseudomonas* spp. and *Xanthomonas* spp. (Büttner 2016; Khan *et al.* 2018), which secrete a variety of effector proteins into host plant cells via the type III secretion system (T3SS). Canonical transcription activator-like (TAL) effectors are common in *Xanthomonas* spp. and serve as model effectors for better understanding disease susceptibility and transcriptional activation (Antony *et al.* 2010; Verdier *et al.* 2012; Cernadas *et al.* 2014; Cohn *et al.* 2014; Hu *et al.* 2014; Cox *et al.* 2017; Phillips *et al.* 2017). Each TAL effector activates transcription by recognizing and binding a specific, largely predictable sequence (effector binding element, EBE) present in the promoter of a targeted *S* gene (Boch *et al.* 2009). Genes encoding the SWEET (Sugars Will Eventually be Exported Transporters) sugar transporters from rice (*Oryza sativa* L.) are some of the best-characterized *S* genes targeted by *Xanthomonas* (Chen *et al.* 2010; Yuan and Wang 2013). The rice genome contains 22 SWEET genes, at least five of which (OsSWEET11–15) are confirmed or predicted *S* genes, playing roles in promoting susceptibility to rice bacterial blight, caused by *X. oryzae* pv. *oryzae* (*Xoo*) (Streubel *et al.* 2013). *Xoo* TAL effectors PthXo1 and PthXo2 activate transcription of OsSWEET11 and OsSWEET13, respectively, while OsSWEET14 is targeted by at least

Received: October 07, 2020. Accepted: January 21, 2021

© The Author(s) 2021. Published by Oxford University Press on behalf of Genetics Society of America.

This is an Open Access article distributed under the terms of the Creative Commons Attribution License (<http://creativecommons.org/licenses/by/4.0/>), which permits unrestricted reuse, distribution, and reproduction in any medium, provided the original work is properly cited.

four TALs (AvrXa7, PthXo3, TalC, and TalF) (Yang and White 2004; Yang et al. 2006; Yu et al. 2011; Yuan et al. 2011; Streubel et al. 2013; Zhou et al. 2015; Doucouré et al. 2018; Tran et al. 2018). Effectors targeting the putative S genes OsSWEET12 and OsSWEET15 have not been identified (Xu et al. 2019). Naturally occurring mutations in the EBEs of OsSWEET11, OsSWEET13, and OsSWEET14 confer resistance to Xoo by preventing their transcriptional activation (Chu et al. 2006; Yang et al. 2006; Yuan et al. 2009; Liu et al. 2011; Hutin et al. 2015; Zhou et al. 2015; Zaka et al. 2018). Recently, the use of TALEN and CRISPR-Cas gene editing techniques to edit SWEET and other S genes has been reported to improve disease resistance in rice (Li et al. 2012; Wang et al. 2016; Blanvillain-Baufumé et al. 2017; Oliva et al. 2019; Xu et al. 2019). Modifications to SWEET genes and other types of S genes have also been successful for improving resistance in pathosystems of citrus (Peng et al. 2017), cucumber (Chandrasekaran et al. 2016), tomato (Nekrasov et al. 2017), wheat (Wang et al. 2014; Zhang et al. 2017), and cassava (Gomez et al. 2019).

Xanthomonas axonopodis pv. *manihotis* (*Xam*) causes cassava bacterial blight (CBB). CBB is a worldwide problem, occurring in all regions where cassava is grown. Severity is extremely variable and unpredictable, sometimes resulting in 100% crop loss (López and Bernal 2012; Lin et al. 2019). No genetic resistance to CBB is available. Symptoms of an infection begin with dark green lesions on leaves (i.e., water soaking), followed by leaf wilting and eventual death of aboveground tissues. Upon infection, *Xam* delivers 20 to 30 effectors via the T3SS into cassava cells, including five TAL effectors (Bart et al. 2012). TAL14 and TAL20 are known to promote virulence by inducing S genes encoding two pectate lyases and a SWEET family sugar transporter, MeSWEET10a, respectively (Cohn et al. 2014; Cohn et al. 2016). Most importantly, ectopic induction of MeSWEET10a in infected cassava leaves is required for the water-soaking phenotype and full pathogen virulence (Cohn et al. 2014).

Understanding how bacterial pathogens manipulate host genes to promote disease at the molecular level is essential for engineering robust, disease-resistant plants. Despite the observed role for MeSWEET10a in susceptibility, it is currently unclear how its induction contributes to disease. During natural infection, *Xam* enters through the stomata or other natural openings, multiplies in leaf tissues, and then spreads systemically through the plant vascular system. It is not known whether induction of MeSWEET10a occurs in all tissue types or if it is limited to specific stages of infection. More generally, the spatial and temporal dynamics of MeSWEET10a induction during natural infections is unknown. To date, the tools required to address these questions have been lacking.

Gene editing technologies can facilitate the development of new tools for non-model organisms. Precise, error-free, knock-in products can be produced from the induction of DNA double-stranded break (DSB) repair pathways. This requires the introduction of a T-DNA that contains CRISPR/Cas9 elements plus a donor repair template. DSB repair is achieved by either of two pathways: either error-prone, non-homologous end-joining (NHEJ), or the more precise homology-directed repair (HDR) pathway, with plant cells generally utilizing NHEJ (Puchta 2005). HDR is well established as an effective way to generate error-free products, but is extremely inefficient in plants, often occurring at rates less than 1% of transformed tissue (Paszowski et al. 1988; Fauser et al. 2012; Hahn et al. 2018; Schmidt et al. 2019).

In this work, we developed a tool that can be used to visualize one of the initial steps of CBB infection *in vivo*. This was done by exploiting the HDR pathway and the transcriptional activation of

MeSWEET10a by TAL20 to generate cassava plants wherein MeSWEET10a was tagged with GFP in its native genomic context. More generally, a time-saving strategy was devised using a tissue-specific transcriptional activator (TA) designed to make the products of successful HDR identifiable early in the process of tissue culture, facilitating this research. Using this strategy, we successfully selected and propagated edited plants to maturity. Furthermore, we re-activated expression of and visualized MeSWEET10a-GFP in regenerated plants, demonstrating their viability as tools for visualizing gene expression changes occurring in *planta*. While CRISPR/Cas9 has been used to successfully generate mutants in cassava (Odipio et al. 2017; Odipio et al. 2018; Mehta et al. 2019; Gomez et al. 2019), to our knowledge this is the first demonstration of CRISPR-mediated HDR and gene tagging *in vivo*.

Materials and Methods

Production of plants and growth conditions

Transgenic cassava lines of cultivar TME 419 were generated and maintained *in vitro* as described previously (Taylor et al. 2012; Chauhan et al. 2015). Briefly, transgenic friable embryogenic callus (FEC) cells were selected for resistance using paromomycin (27.5 μ M) on spread plates (also containing 125 mg/L cefotaxime). On stage 1, 2, and 3 plates, 45 μ M paromomycin was used. Except where indicated, the detection of GFP-derived fluorescence was assessed after three weeks in culture on stage 1, 2, or 3 regeneration media using a Nikon C15304 dissecting microscope equipped with an excitation filter of 460-500 nm and a barrier filter of 510 LP. Growth chamber settings used for tissue culture were 28°C \pm 1°C; 75 μ mol/m²/s light; 16-hr light/8-hr dark. *In vitro* plantlets were propagated and established in soil on a mist bench. Once established, plants were transferred to an open bench in the greenhouse with conditions of 29°C; humidity >50%; 16-hr light/8-hr dark; 1000-W light fixtures supplemented natural light levels below 400 W/m².

gRNA design and plasmids

Guide RNAs were designed to target the 3' end of MeSWEET10a (gene identifier *Manes.06G123400*, *Manihot esculenta* genome v6.1). Sequences that consisted of a 5'-N₍₂₀₎NGG-3' motif were identified using the "Find CRISPR Sites" algorithm of Geneious, version 9.1.8 (Kearse et al. 2012). The software was used to exclude sites with potential off-target activity elsewhere in the cassava genome. The construct containing gRNAs (gRNA1: CATTAACATTACCATTAACG and gRNA2: AGGGACACCAATGTCCTGCT), Cas9 and the repair template was made using a modular system followed by final Golden Gate assembly as described previously (Čermák et al. 2017). Specifically, the final Golden Gate assembly consisted of three modules: pMOD_A0501 (encoding Cas9 and the Csy4 endonuclease), pMOD_B2103 (guide RNAs (gRNAs) separated by Csy4 spacers), pMOD_C0000 (the repair template), and a binary vector backbone (pTRANS_220d). The vector pMOD_A0501 was not modified. Guide RNAs were cloned into pMOD_B2103 using Golden Gate assembly following PCR synthesis of gRNA products using primers TC290-2, TC219, TC220, TC221, TC222, and TC222-2 (Table S1). The repair template (left homology arm (LHA, 866 bp), GFP (789 bp), and right homology arm (RHA, 815 bp)) was amplified using the following primer pairs: LHA (Bael-LHA-F1, Bael-LHA-R1), GFP (Bael-GFP-F2, Bael-GFP-R2), and RHA (Bael-RHA-F3, Bael-RHA-R3) and cloned into pMOD_C0000 using Gibson Assembly[®] (New England BioLabs). Editing of the repair template by Cas9 was prevented by single base pair substitutions

of the PAM sites, generating silent mutations in the coding sequence of the gene. All three final modules (A, B, C) were assembled into the backbone of the binary vector pTRANS_220d using Golden Gate cloning. The TA system was then added to the resulting pTRANS_220d plasmid. The vector was linearized using *Sma*I, and the activator system was added using In-Fusion cloning (In-Fusion[®] HD Cloning Plus, Takara) according to the manufacturer's instructions. For the activator system, a tissue-specific promoter was identified (*Manes.17G095200*) showing high transcriptional activity in FEC cells (http://shiny.danforthcenter.org/cassava_atlas) generated by tissue-specific RNA-seq (Wilson et al. 2017). The Gene Finder tool in Cassava Atlas was used, with the search parameters "on" (FPKM > 300) in FEC, "off" (FPKM < 5) in organized embryogenic structures (OES), and "either" in all other tissue types. PCR (primers 17p-F and 17p-R) was used to amplify 615 bp of the promoter region upstream of the annotated transcriptional start site of the gene (*Manihot esculenta* genome v6.1, <http://phytozome.jgi.doe.gov>). TAL20 from *Xanthomonas axonopodis* pv. *manihotis* (*Xam668*) was amplified by PCR (primers TAL20-F and TAL20-R) for use as the TA of MeSWEET10a. The In-Fusion reaction was performed according to the manufacturer's instructions. All primer sequences are listed in Table S1. The final construct was transformed into electrocompetent *Agrobacterium tumefaciens* strain LBA4404, and positive colonies selected on LB agar plates containing kanamycin (50 µg/ml), rifampicin (100 µg/ml), and streptomycin (30 µg/ml).

Genotyping for HDR

Approximately 100 milligrams of tissue from either *in vitro*-grown plantlets or leaf tissue from greenhouse-grown plants was used for genomic DNA extraction (GenElute[™] Plant Genomic DNA Miniprep Kit, Sigma). PCR was performed using primers SWEET10a_g-F and SWEET10aPro-R (Table S1). For Sanger sequencing, bands were isolated from a gel, subcloned (pCR4-TOPO TA Vector, Thermo Fisher Scientific), and sequenced (standard M13 primers) to verify zygosity and scarless insertion.

MeSWEET10a expression

MeSWEET10-GFP induction: *Xanthomonas* strains were grown on plates containing necessary antibiotics for 2 to 3 days at 30 °C. The *Xanthomonas* strains used and their antibiotic resistances are as follows: (1) *Xam668* (rifampicin 50 µg/ml), (2) *Xam668*ΔTAL20 (suicide vector knockout, tetracycline 5 µg/ml, rifampicin 50 µg/ml) (Cohn et al. 2014), (3) *Xanthomonas evesicatoria* (*Xe*, rifampicin 50 µg/ml), and (4) *Xe*+TAL20_{*Xam668*} (kanamycin 50 µg/ml, rifampicin 50 µg/ml) (Cohn et al. 2014). Bacteria were scraped from the plates into 10 mM MgCl₂ to concentrations of OD_{600nm} = 1. The first fully expanded leaf of each plant was inoculated with a 1 ml needleless syringe using one bacterial strain per lobe and 5 to 10 injection points on each of 2 or 3 leaves. After inoculation, plants were kept under fluorescent light on a 12-hour day/night light cycle at 27 °C for either 3 days (for RNA) or 7 days (for microscopy).

RNA: Three days post-infiltration (dpi), samples were taken using a 7-mm cork borer at each infiltration site, frozen in liquid nitrogen, and ground to a fine powder, and RNA was extracted (Spectrum[™] Plant Total RNA Kit, Sigma). Biological replicates were pooled, such that each RNA sample contained multiple injection sites from 2 or 3 leaves. One microgram of DNase-treated RNA was converted to cDNA (SuperScript[™] III Reverse Transcriptase, Invitrogen) and used for RT-PCR. Details of the PCR cycle numbers and primer sequences are shown in Table S1.

Confocal microscopy: Leaves from plant line #31 were infiltrated with either *Xe* or *Xe*+TAL20_{*Xam668*}, and the abaxial side was

imaged at 7 dpi. Square leaf samples of approximately 2 cm by 2 cm were taken near the infiltration point and mounted in a 35-mm Nunc coverglass bottom dish for microscopy. Confocal images were acquired at 1024x1024 pixel resolution on a Leica SP8-X using an HC PlanApoChromat 63X Water Immersion Objective Lens with the pinhole set to 1 Airy unit. A 488-nm laser was used for excitation to image transmitted light with the spectral prism set to collect 493- to 585-nm and 654- to 779-nm emission wavelengths for GFP and chloroplast autofluorescence, respectively.

MeSWEET10a endogenous expression: Because wild-type (WT) cassava does not flower under our greenhouse conditions, flower tissue was collected from a CRISPR-generated line that has a mutation in the floral-repression pathway (*TERMINAL FLOWER1*, *TFL1*) (Odipio et al. 2018; Adeyemo et al. 2019). RNA was extracted (Spectrum[™] Plant Total RNA Kit, Sigma) from male and female floral tissues. As a positive control for MeSWEET10a expression, WT cassava leaves were infiltrated with *Xe*+TAL20_{*Xam668*} (Cohn et al. 2014), and RNA was extracted at 3 dpi and used for RT-PCR. Primers sequences are listed in Table S1.

Results

Strategy for generating HDR products in cassava

A previous transcriptomics study revealed that MeSWEET10a expression is induced during CBB infection and required for full pathogen virulence (Cohn et al. 2014). However, the spatial and temporal dynamics of MeSWEET10a induction during this process remain unknown. We sought to develop a visual tool for monitoring CBB infection using CRISPR-based gene editing technology to tag MeSWEET10a with GFP at the 3' end of the endogenous locus. The endogenous expression pattern for MeSWEET10a does not lend itself to easy screening for HDR products, as the gene is normally only expressed in flowers (http://shiny.danforthcenter.org/cassava_atlas, Figures 1a, S1). Therefore, we developed the strategy outlined in Figure 1b. The T-DNA transformed into cassava callus tissue contained CRISPR components (the nuclease (Cas9) and gRNAs), a repair template (GFP flanked by homology arms), and a TA component designed to facilitate screening early in the tissue culture process. The TA component consisted of a known TA of MeSWEET10a from *Xam*, TAL20, driven by a tissue-specific promoter (from cassava gene *Manes.17G095200*) that is active primarily during the FEC stage of cassava transformation and propagation (Figure 1c). Thus, the TA system enables high-throughput, nondestructive screening for the tagged gene product (MeSWEET10a-GFP). Because ectopic expression and localization of MeSWEET10a-GFP at the plasma membrane may be detrimental, or even lethal during the tissue culture process, an endoplasmic reticulum (ER) localization signal (HDEL) was included at the C-terminus of GFP in order to sequester the tagged protein (Gomord et al. 1997). The resulting construct (supplemental sequence file 170. pIIICI_8469_17G095200pTAL20) carrying the above components was used to transform FEC derived from cassava cultivar TME 419.

Identification of HDR-positive lines

We used PCR to identify putatively successful products of HDR in which GFP is present at the 3' end of MeSWEET10a. Genotyping plant tissue was carried out using a forward primer that binds the endogenous locus upstream of the LHA (left homology arm, *i.e.*, not included in the repair template) and a reverse primer that either binds GFP or binds just downstream of the MeSWEET10a stop codon (Figure 2a). To estimate a baseline for HDR efficiency

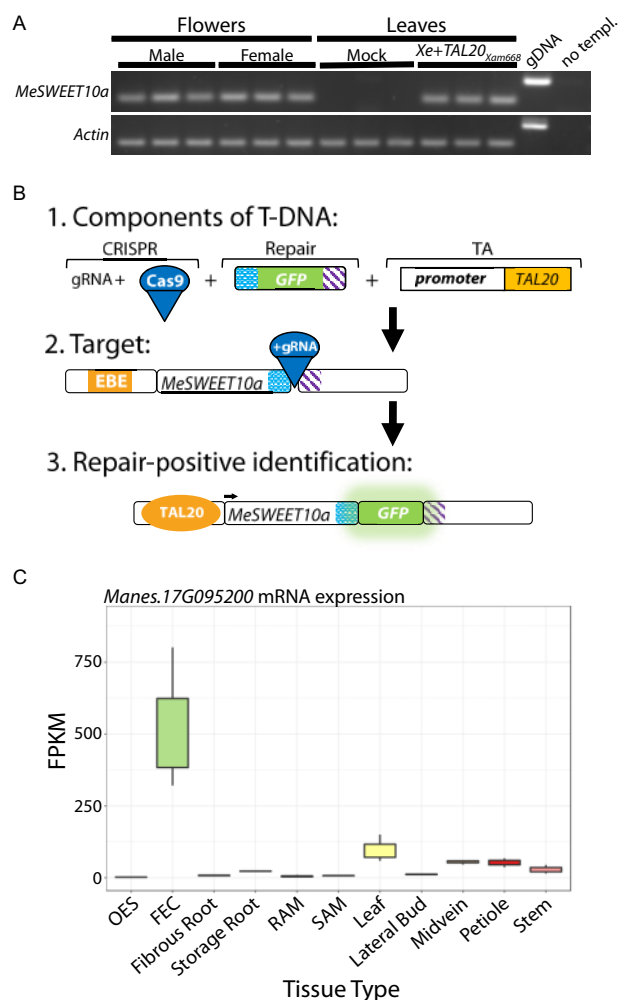


Figure 1 CRISPR-TA-coupled HDR strategy for tagging *MeSWEET10a*. **(a)** RT-PCR for *MeSWEET10a* expression in floral tissue. Analyses of male or female floral tissues are shown separately. *Xe-* and *Xe+TAL20_{Xam668}*-infiltrated leaf tissues, harvested 2 days post-infiltration (dpi), were analyzed as negative or positive controls, respectively. Three biological replicates are presented for each tissue type. *Actin* was used as a loading control. Genomic DNA (gDNA) and no template controls are also shown. **(b)** Summary of the CRISPR-TA-coupled HDR strategy for tagging *MeSWEET10a*. Row 1: the supplied T-DNA includes CRISPR-based gene editing components (gRNA(s) and a nuclease, Cas9), a GFP-containing repair template (homology arms shown in blue/white and purple/white patterns), and a TA system, consisting of a FEC tissue-specific promoter and the *TAL20* gene. Row 2: targeting the 3' end of the *MeSWEET10a* locus. Cas9 + gRNAs cut just before the stop codon. Sequences homologous to the arms of the repair template are indicated in matched colored patterns. The effector binding element (EBE) present in the promoter of *MeSWEET10a* is shown in orange. Row 3: Identification of repair-positive individuals using the TA system. *TAL20* (orange circle) binds the EBE, activating *MeSWEET10a* expression (arrow). If the gene has been tagged in frame with *GFP*, fluorescence is detected through screening. Homology arms remain present (blue/white and purple/white patterns). **(c)** Expression pattern of gene from which the promoter was used in panel B. Y-axis: Fragments per kilobase of transcript per million mapped reads (FPKM) values. X-axis: tissue types included in tissue-specific RNA-seq data (Wilson et al. 2017). OES: organized embryogenic structures, FEC: friable embryogenic callus, SAM: shoot apical meristem, RAM: root apical meristem. Graph was produced using the available online Cassava Atlas tool (http://shiny.danforthcenter.org/cassava_atlas).

in cassava, we performed an experiment wherein we sacrificed tissues early in the tissue culture process, 4 days after co-culture with *Agrobacterium* and after antibiotic selection (Taylor et al. 2012). DNA was extracted from 300 individual clusters (lines) of

healthy, actively proliferating embryogenic callus. This tissue was not screened for visual expression of GFP, and it is not possible to know how many clusters would have subsequently developed to produce plants. Of the 300 lines selected, six were identified as positive for GFP insertion at *MeSWEET10a* using PCR (*MeSWEET10a* forward primer and GFP reverse primer), giving an estimate of HDR efficiency of 2% (Figure 2b). Because all transformed tissues were sacrificed for genotyping, no plant lines were recovered from this experiment.

Next, we investigated whether the TA system and subsequent screening for GFP expression would increase the likelihood of identifying successful HDR. This strategy was advantageous for three reasons: (1) GFP screening is more high-throughput than DNA extraction and PCR; (2) harvesting samples for DNA extraction is destructive and can result in contamination, while GFP screening is relatively risk-free; and (3) the presence of detectable GFP indicates that a translated protein is being produced. Using the TA system, FEC tissue was visually screened for a GFP signal five weeks after transformation, and healthy, proliferating GFP-positive tissues selected during either stage 2 or stage 3 of the process of somatic embryo regeneration (Figure 2c). Screening during stage 2 identified 25 GFP-positive lines. Of these, two were confirmed as successful products of HDR (lines 12 and 42, Figure 2b). Scarless insertion of *GFP* was validated by directly sequencing the PCR product generated using a *MeSWEET10a* forward primer and a *GFP*-specific reverse primer (Figure 2a, primers 171 and 164, Figure S2). Thus, the TA system successfully identified positive products of HDR. Unfortunately, the identified lines did not develop into viable plants. A subsequent round of transformation and GFP screening during stage 3 identified 16 GFP-expressing positive lines. Of these, line #31 was confirmed as a successful HDR event (Figure 2, b and d). The two bands detected by PCR were consistent with a genotype hemizygous for the insertion of *GFP*. Subsequent PCR and sequencing confirmed successful, scarless insertion of *GFP* sequence at the 3' end of *MeSWEET10a* in a hemizygous context (Figure S2). This result is consistent with the fact that successful HDR is relatively rare. In addition, the hemizygous nature of the insertion may have resulted from background heterozygosity at the gRNA target sites. At the start of this project, we designed gRNAs based on available whole-genome re-sequencing data for TME419 as follows: gRNA1: CATTAAACATTACCATTAAACG and gRNA2: AGGGACACCAATGTCCTGCT. However, subsequent Sanger sequencing at this locus from the stock of WT TME 419 cassava plants used for this experiment found that the gRNA2 spacer sequence is a perfect match for only one of the chromosomes, containing 2 mismatches (underlined) to the other copy of *MeSWEET10a*. Additionally, gRNA1 Sanger sequencing data also showed that the intended PAM site for gRNA1 (TGG) was not present (TGA) on either chromosome; thus, this allelic site is not a target for gRNA1. Sequencing of the WT PCR band revealed no evidence of cutting in, or near the targeted sequences, suggesting that the gRNAs may not be able to bind this allele (Figure S2). These factors likely decreased the number of repair events at the targeted locus.

Plants were successfully regenerated from FEC of line #31, clonally propagated, and established in the greenhouse. Line #31 plants were indistinguishable from WT plants, with no deleterious or "off-type" effects observed (Figures 2, e and f). Thus, screening for the GFP signal enabled the identification of a viable, HDR-positive cassava plant line, adding cassava to the list of plants in which HDR-based gene tagging has been achieved. Taken together, we conclude that the tissue-specific TA system,

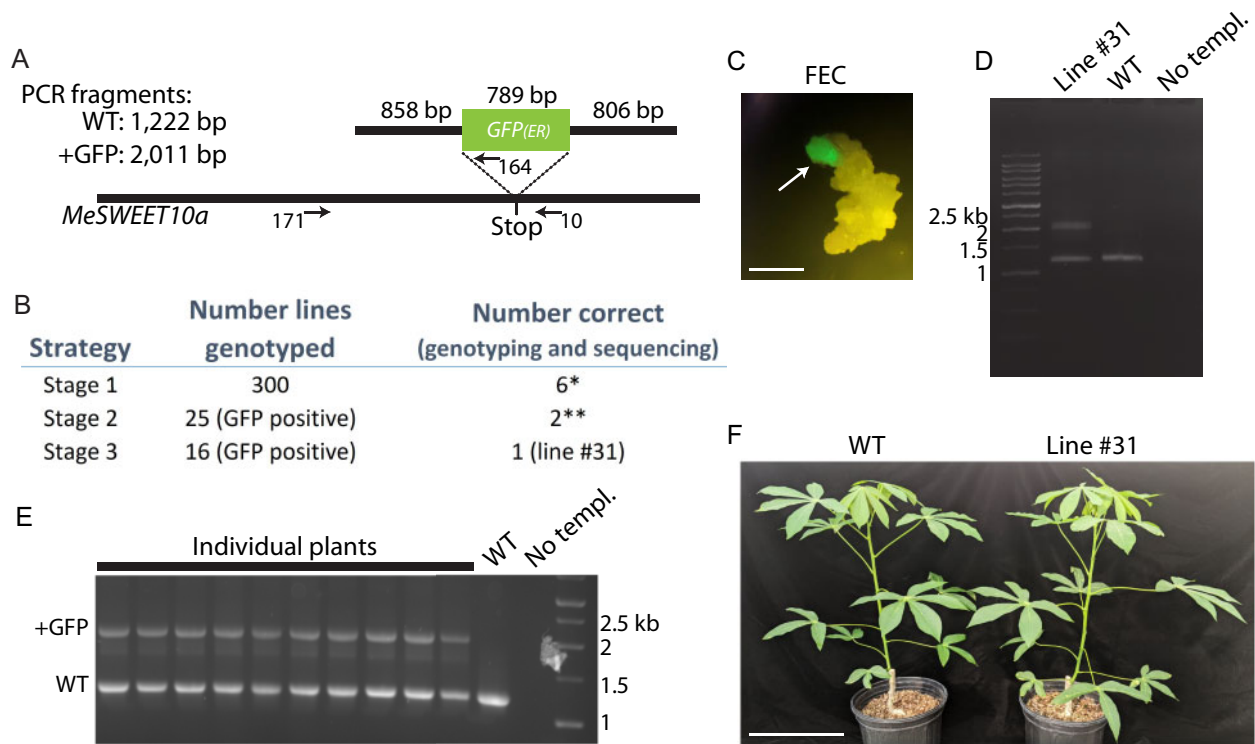


Figure 2 Genotyping and propagation of HDR-positive plants. **(a)** Schematic diagram illustrating the genotyping strategy at the *MeSWEET10a* locus (not drawn to scale). The repair-template with the sizes of the homology arms and *GFP* (with ER-localization signal) is shown above the gene locus. A dotted line illustrates the desired insertion site of *GFP* (just before the stop codon of *MeSWEET10a*). Arrows show approximate locations of primers used. Numbers correspond to primer sequences provided in Table S1. The sizes of PCR products using primers 171 and 10 are given with and without *GFP* integration. **(b)** Table summarizing genotyping from three separate experiments. Row 1: all growing FEC tissue was sacrificed just before stage 1 regeneration. No TA-based screening was performed. Rows 2 and 3: TA-based screening (*GFP* signal) performed for selection at either stage 2 or stage 3 regeneration. *All available tissue was used for genotyping. **Lines died in culture but were confirmed through genotyping and sequencing at the FEC stage (line 12 and 42, Figure S2). **(c)** Example image of epifluorescence signal used for screening *GFP*-positive FEC cells (arrow). Image taken just before stage 1. Scale bar = 1 mm. **(d)** Gel image of PCR products used to identify line #31. Primers 171 and 10 were used to genotype *GFP*-positive FEC tissue. WT, no template (no templ.) controls are shown as well as a size standard with sizes in kilobases (kb) indicated. Bands from the positive line #31 were extracted from a gel and sequenced (Figure S2). **(e)** Same as panel D, but reaction was performed on leaf tissue from propagated plants. **(f)** Greenhouse-grown WT (left) and line #31 (right) adult plants. Scale bar = 25 cm.

coupled with screening at the appropriate stage in tissue culture, facilitated the identification of desired products of HDR. Specifically, this system was used to identify individuals harboring scarless integration of the *GFP* sequence at the 3' end of *MeSWEET10a*.

MeSWEET10a-GFP as a tool for visualizing susceptibility gene expression

Ectopic expression of *MeSWEET10a* driven by *TAL20* is necessary for full virulence of *Xam* (Cohn et al. 2014). Having tagged one of the endogenous copies of *MeSWEET10a* with *GFP*, we next tested whether expression of the fluorescently tagged protein would be induced when *Xanthomonas* delivered *TAL20* into plant cells. Plants were infiltrated with either WT *Xam* or mutant *Xam* wherein *TAL20* had been removed (*Xam*Δ*TAL20*) (Cohn et al. 2014). Additionally, *TAL20* was introduced to another *Xanthomonas* species and was used to test for *MeSWEET10a* induction (*X. euvesicatoria* (*Xe*+*TAL20*_{*Xam668*})) (Cohn et al. 2014). Consistent with previous reports, *MeSWEET10a* was detected in plants infiltrated with either WT *Xam* or *Xe*+*TAL20*_{*Xam668*}, but not detected when infiltrated with bacteria lacking *TAL20* (Figure 3a). To test for expression of the tagged product, a forward primer that binds outside of the LHA was paired with a *GFP* reverse primer and used for RT-PCR (to generate a 677-bp product). A product corresponding to *MeSWEET10a*-*GFP* was detected only in

samples where *TAL20* was present. No transcript was detected in WT plants. Confocal imaging was used to visualize fluorescent protein production in the presence of *TAL20*. *GFP* signal was detected in plants infiltrated with *Xe*+*TAL20*_{*Xam668*} and not WT *Xe* (Figure 3b). The “spider-web” pattern observed in the *GFP*-positive sample is consistent with ER-localized signal (Nelson et al. 2007). This is expected, given the *HDEL* ER-localization signal present in the integrated *GFP* sequence (Gomord et al. 1997). The data demonstrates the viability of this strategy for the creation of a tool for visualization of the induction of *S* genes by pathogens and effectors *in vivo*. Generalizing the strategy could allow researchers to tag nearly any protein of interest in its native genomic context.

Discussion

A major bottleneck exists in our knowledge regarding the process of infection by bacterial pathogens and how they manipulate host genes to promote disease at the molecular level. This knowledge will be essential to guide future efforts aimed at engineering robust, disease-resistant plants. For example, there are major gaps in our basic mechanistic understanding of the interface between the plant and the bacterial cell. Timing and location of effector delivery is not well understood. Are effector proteins capable of traveling cell-to-cell and/or do they act in ways that affect nearby cells? Are all cell layers within an infected plant

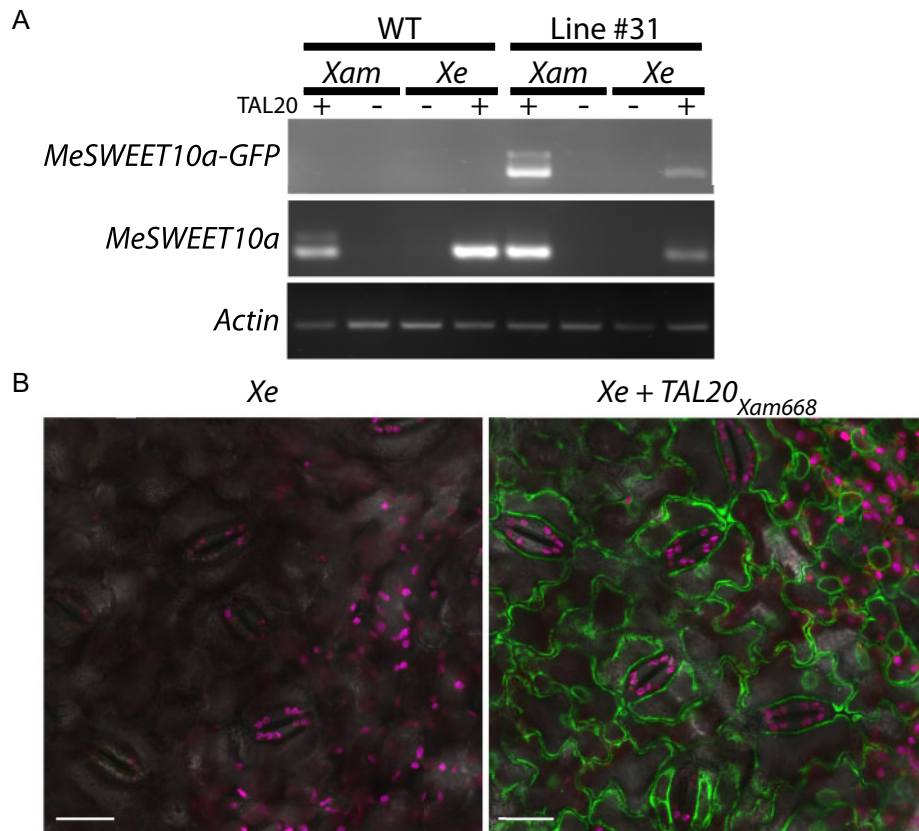


Figure 3 Activation of MeSWEET10a-GFP expression by *Xanthomonas*. **(a)** RT-PCR. Leaves from line #31 were infiltrated with the indicated *Xanthomonas* and RNA extracted at 3 dpi (3 biological replicates per sample). The presence (+) or absence (-) of TAL20 is indicated. Primers specific to MeSWEET10a with GFP were used for the first row and generic MeSWEET10a primers were used for the second row. Actin was used as a loading control. **(b)** Confocal laser scanning microscopy of the abaxial leaf epidermis of *Xanthomonas*-infiltrated leaves. Leaves from line #31 were infiltrated with either Xe or Xe+TAL20_{Xam668} and imaged at 7 dpi. GFP is pseudocolored green, chlorophyll—magenta, and bright field—grey. Scale bar = 20 μ m.

organ (e.g., leaf, stem, root) subjected to the same infection strategy, and if so, are their responses varied? Is infection and subsequent effector delivery a constant process, or is it cyclical, happening in pulses, or in other patterns, possibly informed by environmental cues (e.g., circadian informed by light/dark cycles)? What happens when a plant encounters more than one pathogen at a time?

In this study, we used genome editing techniques to generate cassava plants that serve as tools for studying molecular-level CBB infection dynamics. A strategy was developed to facilitate the identification of successful products of HDR to produce plants harboring MeSWEET10a tagged with sequence encoding a fluorescent protein. This strategy resulted in scarless insertion of functional GFP at the endogenous locus of MeSWEET10a, allowing activation of MeSWEET10a-GFP expression by Xam and, more specifically TAL20_{Xam668}, verified at the transcriptional and translational levels. The ER-localization signal included at the C-terminus of GFP sequesters the tagged protein away from the plasma membrane. However, because the GFP insertion is hemizygous, the plants also contain a copy of MeSWEET10a that should have WT localization. Thus, the plants should be still fully susceptible to CBB.

These plants will serve as a valuable resource, enabling the visualization of S gene activation and CBB infection at the organ, tissue, and molecular levels. However, further development of this tool will still be needed in order to realize its full potential. As shown in Figure 3, both WT Xam and Xe+TAL20_{Xam668} are able to activate the transcription of MeSWEET10a-GFP, yet only

Xe+TAL20_{Xam668} displayed a visible GFP signal in infected tissue. Though performed in parallel, we were unable to detect a clear GFP signal in plants infiltrated with WT Xam. We hypothesize that this could be due to tissue health, given that disease is actively occurring in Xam-infected tissue. Further experimentation with bacterial delivery, concentrations at the infection site and timing of imaging will be needed in order to fully optimize this system for visualizing CBB. Additionally, labeling of the bacteria with a contrasting fluorophore (e. g. RFP) will enable simultaneous visualization of the bacteria and the induction of MeSweet10a-GFP. Model plant systems are often used for tool development due to a relative abundance of resources. Though clearly valuable to the community, such findings or strategies often do not translate to crop systems and can be of limited use outside of the laboratory. Here, we describe a time-saving approach, useful for answering the questions posed above about the mechanisms of plant-pathogen interactions. The work was performed in a non-model system that is also a farmer-preferred cultivar of cassava. Going forward, the development of such tools will be essential for answering detailed questions about disease processes and the timing of infection in this pathosystem. This strategy decreases the number of steps (and consequently the time) from technological development to its real-world impact.

In order to identify the rare, successful products of HDR, we developed an approach combining CRISPR-based genome editing technology with a tissue-specific TA system. It is worth noting that screening during the late stage of somatic embryo

regeneration (stage 3, [Figure 2b](#)) resulted in the regeneration of viable, HDR-positive plants. Although we were able to identify HDR-positive lines earlier in the process of tissue culture, these lines did not reliably regenerate to become mature plants. The data presented for screening at stage 1 in [Figure 2b](#) is intended to provide information addressing the frequency of HDR that is occurring in FEC. Though HDR rates are well known to be low for plants, to our knowledge, no data concerning the rate of HDR in cassava has been published. Therefore, the stage 1 results presented here provide some indication of a baseline for what might be happening at the molecular level in cassava. This work was done within the constraints of the system, and population sizes are not adequate for applying statistics to assess a significant increase in efficiency. Additionally, given the challenges concerning the completeness of the cassava genome and gRNA design, it is likely that efficiency could have been increased with more comprehensive sequence information. The FEC TA system designed for this experiment also resulted in a number of false-positive lines when GFP screening was performed at stage 2 or stage 3. GFP-positive FEC tissue screened and selected at both stages 2 and 3 were not all successful products of HDR ([Figure 2b](#)). Possible explanations for this include: (1) direct expression from the integrated T-DNA, if it had randomly inserted into an actively transcribed region of the genome; (2) false-negative genotyping by PCR (*e.g.*, inefficient amplification or priming sites destroyed); or (3) spontaneous/unintended HR at a different locus that is actively transcribed. Additional experiments will be needed to explore these possible explanations.

The TA-based HDR strategy outlined here presents a powerful approach for additional applications, especially for plant systems, in which HDR is a rare event ([Schmidt et al. 2019](#)). Given the time- and labor-intensive nature of cassava transformation, it is beneficial if successful products are identified early in the process of tissue culture. Because our gene of interest is not normally expressed during the tissue culture process, we chose a FEC-specific promoter driving a well-established TA specific to this gene, TAL20_{Xam668}. However, the true power inherent in this strategy is its adaptability to many other applications and systems, including the following: multiple and/or simultaneous knock-in events (where the rarity of HDR would be an even more limiting factor), epitope tagging, and allele swapping. Any HDR event for which screens or selection may be performed is compatible with this strategy, such as herbicide/antibiotic resistance or pigment production. Additionally, other tissue-specific or inducible TA systems can be employed via the use of an appropriate promoter (*e.g.*, specific to seeds, cotyledons, hypocotyls, floral structures, etc.) coupled with either known or programmable TAs (*e.g.*, dCas9-TV) ([Li et al. 2017](#)). Currently, certain applications of HDR in plant systems are not technically practical and therefore not attempted. It is our hope that the work presented here demonstrates that given a well-designed approach, tools can be developed for the direct study of non-model systems.

Data availability statement

Plant lines and constructs are available upon reasonable request. Table S1 lists the primers used in manuscript. Figure S1 supports [Figure 1](#) and shows the expression pattern of MeSWEET10a in vegetative tissues. Figure S2 supports [Figure 2](#) and shows Sanger sequencing of successful knock-in lines. File 170. pIICI_8469_17 G095200pTAL20 shows the map (pdf) and sequence (gb) of the construct used. Supplemental Material are available at figshare DOI: <https://doi.org/10.25387/g3.13641035>.

Acknowledgements

We are grateful for valuable advice and discussions with members of the Bart and Meyers labs as well as the DDPSC greenhouse staff for their work supporting this study. Additionally, we thank John Odipio for providing floral tissue for gene expression analysis. We acknowledge imaging support from Dr. Kirk Czymmek at the Advanced Bioimaging Center, Donald Danforth Plant Science Center, and usage of the Leica SPX-8 acquired through an NSF Major Research Instrumentation Grant (DBI-1337680).

Funding

This work was supported by the Bill and Melinda Gates Foundation (OPP1125410) and the National Science Foundation (NSF EDGE Award 1827761).

Conflicts of Interest: The authors declare no conflicts of interest.

Literature cited

- Adeyemo OS, Hyde PT, Setter TL. 2019. Identification of FT family genes that respond to photoperiod, temperature and genotype in relation to flowering in cassava (*Manihot esculenta*, Crantz). *Plant Reprod.* 32:181–191. doi:10.1007/s00497-018-00354-5.
- Antony G, Zhou J, Huang S, Li T, Liu B et al. 2010. Rice xa13 recessive resistance to bacterial blight is defeated by induction of the disease susceptibility gene Os-11N3. *Plant Cell.* 22:3864–3876. doi:10.1105/tpc.110.078964.
- Bart R, Cohn M, Kassen A, McCallum EJ, Shybut M et al. 2012. High-throughput genomic sequencing of cassava bacterial blight strains identifies conserved effectors to target for durable resistance. *PNAS.* 109:E1972–E1979. doi:10.1073/pnas.1208003109.
- Blanvillain-Baufumé S, Reschke M, Solé M, Auguy F, Doucoure H et al. 2017. Targeted promoter editing for rice resistance to *Xanthomonas oryzae* pv. *oryzae* reveals differential activities for SWEET14-inducing TAL effectors. *Plant Biotechnol J.* 15:306–317. doi:10.1111/pbi.12613.
- Boch J, Scholze H, Schornack S, Landgraf A, Hahn S et al. 2009. Breaking the code of DNA binding specificity of TAL-type III effectors. *Science.* 326:1509–1512. doi:10.1126/science.1178811.
- Brown JKM. 2015. Durable resistance of crops to disease: a Darwinian perspective. *Annu Rev Phytopathol.* 53:513–539. doi:10.1146/annurev-phyto-102313-045914.
- Büttner D. 2016. Behind the lines—actions of bacterial type III effector proteins in plant cells. *FEMS Microbiol Rev.* 40:894–937. doi:10.1093/femsre/fuw026.
- Čermák T, Curtin SJ, Gil-Humanes J, Čegan R, Kono TJY et al. 2017. A multipurpose toolkit to enable advanced genome engineering in plants. *Plant Cell.* 29:1196–1217. doi:10.1105/tpc.16.00922.
- Cernadas RA, Doyle EL, Niño-Liu DO, Wilkins KE, Bancroft T et al. 2014. Code-assisted discovery of TAL effector targets in bacterial leaf streak of rice reveals contrast with bacterial blight and a novel susceptibility gene. *PLOS Pathog.* 10:e1003972. doi:10.1371/journal.ppat.1003972.
- Chandrasekaran J, Brumin M, Wolf D, Leibman D, Klap C et al. 2016. Development of broad virus resistance in non-transgenic cucumber using CRISPR/Cas9 technology. *Mol Plant Pathol.* 17:1140–1153. doi:10.1111/mpp.12375.
- Chauhan RD, Beyene G, Kalyaeva M, Fauquet CM, Taylor N. 2015. Improvements in Agrobacterium-mediated transformation of cassava (*Manihot esculenta* Crantz) for large-scale production of

- transgenic plants. *Plant Cell Tiss Organ Cult.* 121:591–603. doi:10.1007/s11240-015-0729-z.
- Chen L-Q, Hou B-H, Lalonde S, Takanaga H, Hartung ML et al. 2010. Sugar transporters for intercellular exchange and nutrition of pathogens. *Nature.* 468:527–532. doi:10.1038/nature09606.
- Chu Z, Yuan M, Yao J, Ge X, Yuan B et al. 2006. Promoter mutations of an essential gene for pollen development result in disease resistance in rice. *Genes Dev.* 20:1250–1255. doi:10.1101/gad.1416306.
- Cohn M, Bart RS, Shybut M, Dahlbeck D, Gomez M et al. 2014. *Xanthomonas axonopodis* virulence is promoted by a transcription activator-like effector-mediated induction of a SWEET sugar transporter in cassava. *MPMI.* 27:1186–1198. doi:10.1094/MPMI-06-14-0161-R.
- Cohn M, Morbitzer R, Lahaye T, Staskawicz BJ. 2016. Comparison of gene activation by two TAL effectors from *Xanthomonas axonopodis* pv. *manihotis* reveals candidate host susceptibility genes in cassava. *Mol Plant Pathol.* 17:875–889. doi:10.1111/mpm.12337.
- Cox KL, Meng F, Wilkins KE, Li F, Wang P et al. 2017. TAL effector driven induction of a SWEET gene confers susceptibility to bacterial blight of cotton. *Nat Commun.* 8:1–14. doi:10.1038/ncomms15588.
- Dangl JL, Horvath DM, Staskawicz BJ. 2013. Pivoting the plant immune system from dissection to deployment. *Science.* 341:746–751. doi:10.1126/science.1236011.
- Doucouré H, Pérez-Quintero AL, Reshetnyak G, Tekete C, Auguy F et al. 2018. Functional and genome sequence-driven characterization of tal effector gene repertoires reveals novel variants with altered specificities in closely related malian *Xanthomonas oryzae* pv. *oryzae* strains. *Front Microbiol.* 9:1657. doi:10.3389/fmicb.2018.01657.
- Fausser F, Roth N, Pacher M, Ilg G, Sánchez-Fernández R et al. 2012. In planta gene targeting. *PNAS.* 109:7535–7540. doi:10.1073/pnas.1202191109.
- Feng F, Zhou J-M. 2012. Plant-bacterial pathogen interactions mediated by type III effectors. *Curr Opin Plant Biol.* 15:469–476. doi:10.1016/j.pbi.2012.03.004.
- Gomez MA, Lin ZD, Moll T, Chauhan RD, Hayden L et al. 2019. Simultaneous CRISPR/Cas9-mediated editing of cassava eIF4E isoforms nCBP-1 and nCBP-2 reduces cassava brown streak disease symptom severity and incidence. *Plant Biotechnol J.* 17:421–434. doi:10.1111/pbi.12987.
- Gomord V, Denmat LA, Fitchette-Lainé AC, Satiat-Jeunemaitre B, Hawes C et al. 1997. The C-terminal HDEL sequence is sufficient for retention of secretory proteins in the endoplasmic reticulum (ER) but promotes vacuolar targeting of proteins that escape the ER. *Plant J.* 11:313–325. doi:10.1046/j.1365-313x.1997.11020313.x.
- Hahn F, Eisenhut M, Mantegazza O, Weber APM. 2018. Homology-directed repair of a defective glabrous gene in *Arabidopsis* with Cas9-based gene targeting. *Front Plant Sci.* 9:424. doi:10.3389/fpls.2018.00424.
- Hogenhout SA, Van der Hoorn RAL, Terauchi R, Kamoun S. 2009. Emerging concepts in effector biology of plant-associated organisms. *MPMI.* 22:115–122. doi:10.1094/MPMI-22-2-0115.
- Hu Y, Zhang J, Jia H, Sosso D, Li T et al. 2014. Lateral organ boundaries 1 is a disease susceptibility gene for citrus bacterial canker disease. *PNAS.* 111:E521–E529. doi:10.1073/pnas.1313271111.
- Hutin M, Sabot F, Ghesquière A, Koebnik R, Szurek B. 2015. A knowledge-based molecular screen uncovers a broad-spectrum OsSWEET14 resistance allele to bacterial blight from wild rice. *Plant J.* 84:694–703. doi:10.1111/tpj.13042.
- Kearse M, Moir R, Wilson A, Stones-Havas S, Cheung M et al. 2012. Geneious basic: an integrated and extendable desktop software platform for the organization and analysis of sequence data. *Bioinformatics.* 28:1647–1649. doi:10.1093/bioinformatics/bts199.
- Khan M, Seto D, Subramaniam R, Desveaux D. 2018. Oh, the places they'll go! A survey of phytopathogen effectors and their host targets. *Plant J.* 93:651–663. doi:10.1111/tpj.13780.
- Li T, Liu B, Spalding MH, Weeks DP, Yang B. 2012. High-efficiency TALEN-based gene editing produces disease-resistant rice. *Nat Biotechnol.* 30:390–392. doi:10.1038/nbt.2199.
- Li Z, Zhang D, Xiong X, Yan B, Xie W et al. 2017. A potent Cas9-derived gene activator for plant and mammalian cells. *Nat Plants.* 3:930–936. doi:10.1038/s41477-017-0046-0.
- Lin ZJD, Taylor NJ, Bart R. 2019. Engineering disease-resistant cassava. *Cold Spring Harb Perspect Biol.* 11:a034595. doi:10.1101/cshperspect.a034595.
- Liu Q, Yuan M, Zhou Y, Li X, Xiao J et al. 2011. A paralog of the MtN3/saliva family recessively confers race-specific resistance to *Xanthomonas oryzae* in rice. *Plant Cell Environ.* 34:1958–1969. doi:10.1111/j.1365-3040.2011.02391.x.
- López CE, Bernal AJ. 2012. Cassava bacterial blight: using genomics for the elucidation and management of an old problem. *Tropical Plant Biol.* 5:117–126. doi:10.1007/s12042-011-9092-3.
- Mehta D, Stürchler A, Anjanappa RB, Zaidi SS-A, Hirsch-Hoffmann M et al. 2019. Linking CRISPR-Cas9 interference in cassava to the evolution of editing-resistant geminiviruses. *Genome Biol.* 20:80. doi:10.1186/s13059-019-1678-3.
- Nekrasov V, Wang C, Win J, Lanz C, Weigel D et al. 2017. Rapid generation of a transgene-free powdery mildew resistant tomato by genome deletion. *Sci Rep.* 7:482. doi:10.1038/s41598-017-00578-x.
- Nelson BK, Cai X, Nebenführ A. 2007. A multicolored set of in vivo organelle markers for co-localization studies in *Arabidopsis* and other plants. *Plant J.* 51:1126–1136. doi:10.1111/j.1365-313X.2007.03212.x.
- Odipto J, Alicai T, Ingelbrecht I, Nusinow DA, Bart R et al. 2017. Efficient CRISPR/Cas9 genome editing of phytoene desaturase in cassava. *Front Plant Sci.* 8:doi:10.3389/fpls.2017.01780. [accessed 2020 Sep 17]. <https://www.frontiersin.org/articles/10.3389/fpls.2017.01780/full>.
- Odipto J, Alicai T, Nusinow D, Bart R, Taylor N. 2018. CRISPR/Cas9-mediated disruption of multiple TFL1-like floral repressors activates flowering in cassava. *In Vitro Cellular & Developmental Biology-Animal*, Vol. 54. NEW YORK, NY: SPRINGER. p. S47–S47.
- Oliva R, Ji C, Atienza-Grande G, Huguet-Tapia JC, Perez-Quintero A et al. 2019. Broad-spectrum resistance to bacterial blight in rice using genome editing. *Nat Biotechnol.* 37:1344–1350. doi:10.1038/s41587-019-0267-z.
- Paszkowski J, Baur M, Bogucki A, Potrykus I. 1988. Gene targeting in plants. *Embo J.* 7:4021–4026.
- Peng A, Chen S, Lei T, Xu L, He Y et al. 2017. Engineering canker-resistant plants through CRISPR/Cas9-targeted editing of the susceptibility gene CsLOB1 promoter in citrus. *Plant Biotechnol J.* 15:1509–1519. doi:10.1111/pbi.12733.
- Phillips AZ, Berry JC, Wilson MC, Vijayaraghavan A, Burke J et al. 2017. Genomics-enabled analysis of the emergent disease cotton bacterial blight. *PLOS Genet.* 13:e1007003. doi:10.1371/journal.pgen.1007003.
- Puchta H. 2005. The repair of double-strand breaks in plants: mechanisms and consequences for genome evolution. *J Exp Bot.* 56:1–14. doi:10.1093/jxb/eri025.
- van Schie CCN, Takken FLW. 2014. Susceptibility genes 101: how to be a good host. *Annu Rev Phytopathol.* 52:551–581. doi:10.1146/annurev-phyto-102313-045854.

- Schmidt C, Pacher M, Puchta H. 2019. DNA break repair in plants and its application for genome engineering. In: S Kumar, P Barone, M Smith, editors. *Transgenic Plants: Methods and Protocols*. New York, NY: Springer. p. 237–266.
- Streubel J, Pesce C, Hutin M, Koebnik R, Boch J et al. 2013. Five phylogenetically close rice SWEET genes confer TAL effector-mediated susceptibility to *Xanthomonas oryzae* pv. *oryzae*. *New Phytol.* 200:808–819. doi:10.1111/nph.12411@10.1002/(ISSN)1469-8137 (CAT)VirtualIssues(VI)Phytopathogeneffectorproteins.
- Taylor N, Gaitán-Solís E, Moll T, Trauterman B, Jones T et al. 2012. A high-throughput platform for the production and analysis of transgenic cassava (*Manihot esculenta*) plants. *Tropical Plant Biol.* 5:127–139. doi:10.1007/s12042-012-9099-4.
- Tran TT, Pérez-Quintero AL, Wonni I, Carpenter SCD, Yu Y et al. 2018. Functional analysis of African *Xanthomonas oryzae* pv. *oryzae* TALomes reveals a new susceptibility gene in bacterial leaf blight of rice. *PLoS Pathog.* 14:e1007092. doi:10.1371/journal.ppat.1007092.
- Verdier V, Triplett LR, Hummel AW, Corral R, Cernadas RA et al. 2012. Transcription activator-like (TAL) effectors targeting OsSWEET genes enhance virulence on diverse rice (*Oryza sativa*) varieties when expressed individually in a TAL effector-deficient strain of *Xanthomonas oryzae*. *New Phytol.* 196:1197–1207. doi:10.1111/j.1469-8137.2012.04367.x.
- Wang F, Wang C, Liu P, Lei C, Hao W et al. 2016. Enhanced rice blast resistance by CRISPR/Cas9-targeted mutagenesis of the ERF transcription factor gene OsERF922. *PLoS One.* e0154027.11:doi:10.1371/journal.pone.0154027. [accessed 2020 Feb 6]. <https://www.ncbi.nlm.nih.gov/pmc/articles/PMC4846023/>.
- Wang Y, Cheng X, Shan Q, Zhang Y, Liu J et al. 2014. Simultaneous editing of three homoeoalleles in hexaploid bread wheat confers heritable resistance to powdery mildew. *Nat Biotechnol.* 32:947–951. doi:10.1038/nbt.2969.
- Wilson MC, Mutka AM, Hummel AW, Berry J, Chauhan RD et al. 2017. Gene expression atlas for the food security crop cassava. *New Phytol.* 213:1632–1641. doi:10.1111/nph.14443.
- Xu Z, Xu X, Gong Q, Li Z, Li Y et al. 2019. Engineering broad-spectrum bacterial blight resistance by simultaneously disrupting variable TALE-binding elements of multiple susceptibility genes in rice. *Mol Plant.* 12:1434–1446. doi:10.1016/j.molp.2019.08.006.
- Yang B, Sugio A, White FF. 2006. Os8N3 is a host disease-susceptibility gene for bacterial blight of rice. *PNAS.* 103:10503–10508. doi:10.1073/pnas.0604088103.
- Yang B, White FF. 2004. Diverse members of the AvrBs3/PthA family of type III effectors are major virulence determinants in bacterial blight disease of rice. *MPMI.* 17:1192–1200. doi:10.1094/MPMI.2004.17.11.1192.
- Yu Y, Streubel J, Balzergue S, Champion A, Boch J et al. 2011. Colonization of rice leaf blades by an African strain of *Xanthomonas oryzae* pv. *oryzae* depends on a new TAL effector that induces the rice nodulin-3 Os11N3 gene. *MPMI.* 24:1102–1113. doi:10.1094/MPMI-11-10-0254.
- Yuan M, Chu Z, Li X, Xu C, Wang S. 2009. Pathogen-induced expression loss of function is the key factor in race-specific bacterial resistance conferred by a recessive R gene xa13 in rice. *Plant Cell Physiol.* 50:947–955. doi:10.1093/pcp/pcp046.
- Yuan M, Wang S. 2013. Rice MtN3/saliva/SWEET family genes and their homologs in cellular organisms. *Mol Plant.* 6:665–674. doi:10.1093/mp/sst035.
- Yuan T, Li X, Xiao J, Wang S. 2011. Characterization of *Xanthomonas oryzae*-responsive cis-acting element in the promoter of rice race-specific susceptibility gene Xa13. *Molecular Plant.* 4:300–309. doi:10.1093/mp/ssq076.
- Zaka A, Grande G, Coronejo T, Quibod IL, Chen C-W et al. 2018. Natural variations in the promoter of OsSWEET13 and OsSWEET14 expand the range of resistance against *Xanthomonas oryzae* pv. *oryzae*. *PLoS One.* 13:e0203711. doi:10.1371/journal.pone.0203711.
- Zhang Y, Bai Y, Wu G, Zou S, Chen Y et al. 2017. Simultaneous modification of three homoeologs of TaEDR1 by genome editing enhances powdery mildew resistance in wheat. *Plant J.* 91:714–724. doi:10.1111/tj.13599.
- Zhou J, Peng Z, Long J, Sosso D, Liu B et al. 2015. Gene targeting by the TAL effector PthXo2 reveals cryptic resistance gene for bacterial blight of rice. *Plant J.* 82:632–643. doi:10.1111/tj.12838.

Communicating editor: S. M. Smith